

1

# Economic Damages of Delayed Climate Action

2

By KENT D. DANIEL, ROBERT B. LITTERMAN, AND GERNOT WAGNER\*

3

Draft: January 7, 2026

4

*Delayed climate mitigation imposes substantial economic costs by shifting the burden of adjustment onto future generations. We quantify these welfare losses within a climate-economy model that allows us to calculate the dead-weight loss (DWL) of underpricing carbon pollution. We simulate policy delay by constraining initial mitigation years and comparing resulting welfare outcomes to an unconstrained baseline. We show analytically that delay raises the required expected entry carbon price. Across scenarios, expected re-entry prices are higher by roughly 0.4-0.9% per additional year of delay. The consumption-equivalent DWL even for short delays of 5 to 15 years ranges from 14-32% of first-period consumption, or roughly \$8-19 trillion (2020 USD) in one-time compensation. DWLs rise steeply but concavely in the length of delay, reflecting catch-up pricing and abatement once the constraint lifts.*

*JEL: D62, G12, Q54*

*Keywords: climate risk, climate policy, cost of carbon*

5

Climate economics is, at its core, the economics of delaying optimal choice. Con-  
6 sequences of delaying climate mitigation are profound and quantifiable, as every  
7 year without meaningful reductions in greenhouse gas emissions increases their  
8 concentration and commits the world to higher temperature and greater climate  
9 damages. From an economic perspective, these delays are an implicit transfer of

\* Daniel: Columbia Business School, New York, NY 10027; Litterman: Kepos Capital, New York, NY 10036; Wagner: Columbia Business School, New York, NY 10027; gwagner@columbia.edu. We thank Theo Moers for excellent research assistance, and participants in the 2025 Dialogues in Complexity Workshop at Princeton University for thoughtful comments.

10 welfare from future generations to the present, an intertemporal reallocation that  
11 is driven not by efficiency but political and institutional frictions. Understanding  
12 the dynamics of this delay and quantifying the resulting dead-weight loss (DWL)  
13 is essential in understanding the true cost of inaction.

14 Most climate-economic integrated assessment models (IAMs) seek to identify  
15 the optimal mitigation path that maximizes intertemporal social welfare under  
16 a set of assumed parameters. Yet governments rarely, if ever, follow the paths  
17 that economists identify as socially optimal. Corporate lobbying (Oreskes and  
18 Conway, 2011) and other interest-group politics (Mildenberger, 2020), in part via  
19 public opinion (Dechezleprêtre et al., 2025; Mildenberger and Tingley, 2019), in-  
20 stitutional constraints (Bertram et al., 2024), behavioral barriers (Wagner and  
21 Zeckhauser, 2012), and other political economy considerations (Meckling, Sterner  
22 and Wagner, 2017; Meckling, 2025) defer action, even when — or perhaps espe-  
23 cially when — the social planner’s problem is well understood.<sup>1</sup>

24 The more explicit the attempt at pricing the negative climate externality, the  
25 louder are the voices of vested interests lobbying against climate policy. This  
26 delay in climate action moves the world further off the efficient frontier, which  
27 does not just lead to greater economic damages reflected in higher social cost of  
28 carbon (SCC) calculations (Moore et al., 2024), but in measurable DWLs.

29 Here we examine these costs explicitly. Building on a carbon asset pricing  
30 framework (Bauer, Prostosescu and Wagner, 2024), which extends the Epstein–Zin–  
31 recursive preference structure of Daniel, Litterman and Wagner (2019), we quan-  
32 tify DWLs of delaying optimal policy by comparing carbon price paths under  
33 constrained and unconstrained conditions, analyzing sensitivities of various model  
34 parameters, including technological progress and learning. In contrast to Daniel,  
35 Litterman and Wagner (2019), we further show that the optimal expected carbon  
36 price in a delayed scenario will be higher under standard assumptions than in an

<sup>1</sup>It is also what makes *ex-post* analyses of existing policies so fraught (Stechemesser et al., 2024): Policies that get enacted are necessarily limited in scope and strength.

37 unconstrained scenario.

38 We present simple heuristics about the high and quickly accumulating costs of  
 39 delayed climate action, finding DWLs of delay of between 14-32% of first-period  
 40 consumption, or \$8-19 trillion (2020 USD), even for relatively short delays of  
 41 between 5 and 15 years. These numbers compare to cost estimates of between  
 42 \$400 and \$900 per U.S. household per year, or about \$50 to \$110 billion per year  
 43 for the United States (Clausing, Knittel and Wolfram, 2025) and are significantly  
 44 higher than typically calculated, using SCC-based measures. The optimal carbon  
 45 price in our base case here is roughly \$200, above the median value of around \$185  
 46 of Moore et al. (2024)'s "synthetic distribution" yet well below its mean SCC of  
 47 around \$280. Meanwhile, Bilal and Käenzig (2025) calculate an SCC above \$1500  
 48 and a welfare cost of (only) around 30%. A key difference to our analysis: we  
 49 solve for the 'optimal' carbon price by considering marginal disutility of damages,  
 50 instead of calculating the SCC, the discounted value of the stream of expected  
 51 future damages.

52 **I. Socio-economic modeling choices**

53 To explore how postponing climate policy affects welfare and the socially opti-  
 54 mal carbon price path, we endow a representative agent with recursive Epstein-  
 55 Zin (EZ) preferences and place it within a binomial decision tree where utility  
 56 is maximized at each step. Such preferences allow us to disentangle risk over  
 57 time from risk across states of nature. This distinction follows Epstein and Zin  
 58 (1989, 1991), with a long history in financial economics, and a more recent one  
 59 in modeling the financial implications of climate risks (Ackerman, Stanton and  
 60 Bueno, 2013; Traeger, 2014; Lemoine and Traeger, 2014).

61 The representative agent's preferences follow the recursive Epstein-Zin specifi-  
 62 cation,

$$(1) \quad U_t = \left( (1 - \beta) c_t^\rho + \beta [\mathbb{E}_t(U_{t+1}^\alpha)]^{\rho/\alpha} \right)^{1/\rho},$$

63 where  $\beta := (1 + \delta)^{-1} > 0$  is the one-year discount factor, with  $\delta > 0$  denoting the  
 64 pure rate of time preference (PRTP);  $c_t > 0$  is consumption at time  $t$ ;  $\rho := 1 - 1/\sigma$ ,  
 65 where  $\sigma > 0$  is the elasticity of intertemporal substitution (EIS); and  $\alpha := 1 - \gamma$ ,  
 66 where  $\gamma > 0$  is the coefficient of relative risk aversion (RA). The term  $\mathbb{E}_t(U_{t+1}^\alpha)$   
 67 represents the certainty equivalent of future utility.

68 When  $\alpha = \rho$ , that is, when risk aversion and intertemporal substitution coincide,  
 69 the recursive formulation in Equation (1) collapses to the standard time-  
 70 additive expected-utility form with constant relative risk aversion.

71 For the terminal period  $T$ , we assume exogenous consumption growth  $g > 0$   
 72 and define terminal utility as

$$(2) \quad U_T = \left[ \frac{1 - \beta}{1 - \beta(1 + g)^\rho} \right]^{1/\rho} c_T.$$

73 This specification cleanly separates two central preference parameters:  $\sigma$ , which  
 74 governs willingness to substitute consumption over time, and  $\gamma$ , which governs  
 75 aversion to risk across uncertain future states.<sup>2</sup>

## 76 II. Optimization

77 Following Daniel, Litterman and Wagner (2019) and Bauer, Proistosescu and  
 78 Wagner (2024), we embed the representative agent in a finite-horizon probability  
 79 landscape. Our model has six decision times  $T_0, \dots, T_5$  (Figure 1). At every  
 80 node  $(t, s)$  of the tree, the agent maximizes EZ utility in (1) and chooses a node-  
 81 specific mitigation level  $m_{t,s} \in [0, \bar{m}]$  with upper mitigation bound  $\bar{m}$ , subject to  
 82 climate dynamics, resource constraints, abatement costs, climate damages, and  
 83 the technological feasibility of mitigation. Each choice commits the agent to a  
 84 continuation policy for all downstream nodes in a given branch.

85 The climate state evolves according to the impulse response function (IRF) of  
 86 Joos et al. (2013) for atmospheric CO<sub>2</sub> concentration  $C$  and the TCRE map-

<sup>2</sup>See Appendix A.A1 for parameter values used in our main specification.

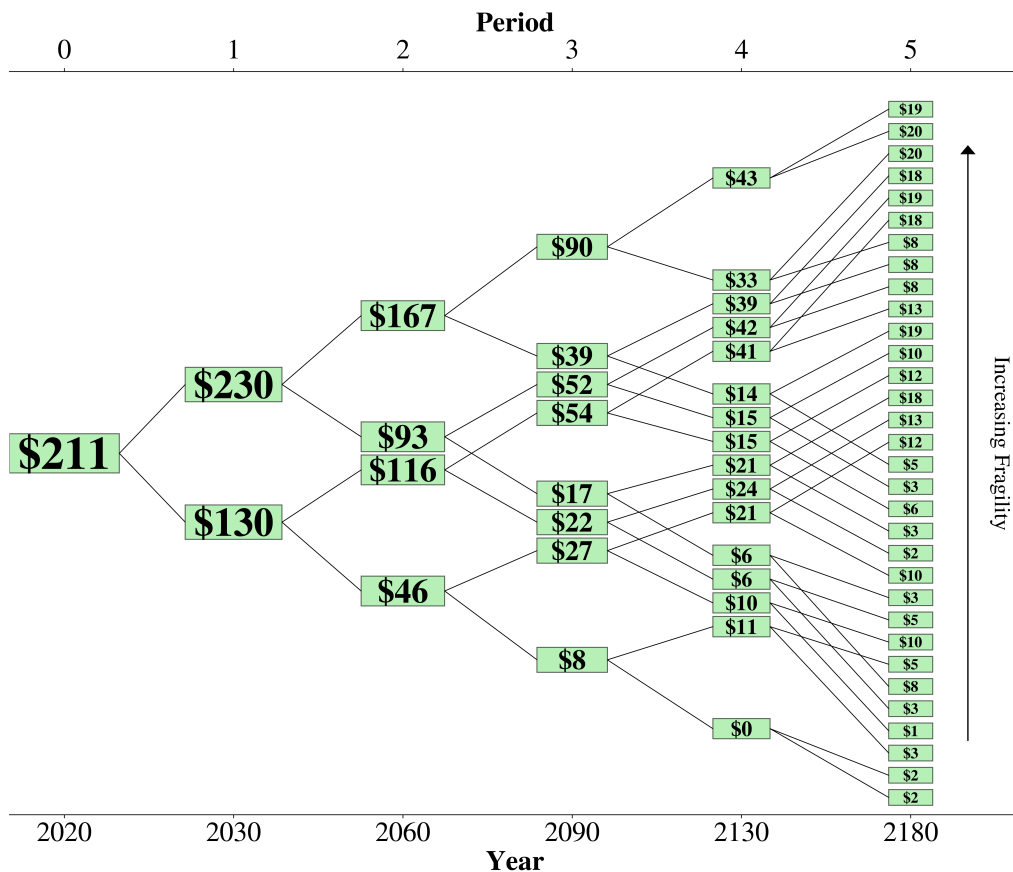


Figure 1. : Optimal price paths (unconstrained baseline)

*Note:* The binomial non-recombining tree shows the optimal node-level shadow-price trajectory on the stochastic decision tree used in the model. Each node represents a shadow price (in 2020 USD per ton CO<sub>2</sub>) at the beginning of the indicated year, conditional on previous realizations of climate and economic uncertainty.

87 ping from cumulative emissions to the global mean surface *temperature anomaly*  
 88  $\theta$  (in  $^{\circ}\text{C}$  above preindustrial), see Eqs. (A2)–(A3) in Appendix A.A1. Our im-  
 89 plementation uses a carbon cycle model with persistent parameters from Joos  
 90 et al. (2013) and uncertain effective TCRE  $\lambda_{\text{eff}} \sim \mathcal{N}(0.52, 0.21^2)$ . For analytical  
 91 results we employ a stylized finite-dimensional representation that preserves the  
 92 key monotonicity properties.

93 Define at node  $(t, s)$  the marginal willingness to pay  $\Phi_{t,s}(\theta_{t,s})$  to avoid one  
 94 additional ton of CO<sub>2</sub> emitted in  $[T_t, T_{t+1})$ . Mitigation has node-specific marginal  
 95 cost  $\kappa'_{t,s}(m_{t,s}, L_{t,s}) = \partial \kappa_{t,s}(m_{t,s}, L_{t,s}) / \partial m_{t,s}$ .

96 At decision time  $t$ , let  $\mathcal{S}_t$  denote the set of nodes (states) and  $\{\pi_{t,s}\}_{s \in \mathcal{S}_t}$  the  
 97 probabilities of those nodes, conditional on information at the start of period  $t$ .  
 98 For any node-level variable  $x_{t,s}$ <sup>3</sup>, write its cross-node expectation as

$$(3) \quad x_t := \mathbb{E}_t [x_{t,S}] = \sum_{s \in \mathcal{S}_t} \pi_{t,s} x_{t,s}.$$

99 We summarize period  $t$  by the expected objects  $\Phi_t := \mathbb{E}_t[\Phi_{t,S}]$  and  $\kappa'_t := \mathbb{E}_t[\kappa'_{t,S}]$   
 100 when needed (using (3)).

101 The climate state at node  $(t, s)$  is  $(C_{t,s}, \theta_{t,s})$ , with  $C_{t,s}$  and  $\theta_{t,s}$  generated by  
 102 Eqs. (A2)–(A3). Period- $t$  expectations are  $C_t := \mathbb{E}_t[C_{t,S}]$  and  $\theta_t := \mathbb{E}_t[\theta_{t,S}]$ . On  
 103 the cost side, mitigation has node-specific marginal cost  $\kappa'_{t,s}(m_{t,s}, L_{t,s})$ , where  $L_{t,s}$   
 104 indexes both exogenous technological progress and endogenous learning-by-doing.  
 105 Past mitigation lowers future costs by shifting down the marginal cost curve.

106 **III. Carbon price paths under delay**

107 To test the cost of delay, we impose a zero-mitigation constraint for the first  
 108 decision node and vary the length  $L$  of that period by shifting the initial decision  
 109 time between 5, 10, and 15 years:  $L \in \{5, 10, 15\}$ . Each constrained run is then  
 110 evaluated against two baseline scenarios, depending on the figure—the optimal

3Subscript  $(t, s)$  denotes a node-level object; subscript  $t$  alone denotes its period- $t$  expectation across  
 $s \in \mathcal{S}_t$  with weights  $\pi_{t,s}$ .

111 expected price at the same  $L$ , and one common  $L = 10$  baseline. Figure 2 shows  
 112 the resulting optimal carbon price paths in expectation over time. We here find  
 113 that the carbon price paths in expectation of each delayed scenario lie above the  
 114 baseline scenario's levels.<sup>4</sup>

115 If the optimum at time  $T_t$  is interior (i.e.,  $m_{t,s}^* \in (0, \bar{m})$  for all  $s \in \mathcal{S}_t$ ) and  
 116 baseline emissions  $E_t > 0$ , the first-order condition at each node equates the  
 117 node-specific marginal abatement cost to the node-specific marginal damage:

$$(4) \quad \tau_{t,s} := \kappa'_{t,s} \left( m_{t,s}^*(\theta_{t,s}, L_{t,s}), L_{t,s} \right) = \Phi_{t,s}(\theta_{t,s}), \quad s \in \mathcal{S}_t.$$

118 where  $\kappa'_{t,s}(m_{t,s}, L_{t,s}) = \partial \kappa_{t,s} / \partial m_{t,s}$ . We summarize the decision period by the  
 119 expected carbon price,

$$(5) \quad \tau_t := \mathbb{E}_t[\tau_{t,S}] = \mathbb{E}_t[\Phi_{t,S}(\theta_{t,S})] = \sum_{s \in \mathcal{S}_t} \pi_{t,s} \Phi_{t,s}(\theta_{t,s}),$$

120 which is the probability-weighted average across all nodes at time  $t$ . Learning-by-doing and exogenous technological progress enter through  $L_{t,s}$ , shifting  
 121  $\kappa'_{t,s}$  and thereby altering both the node-level prices  $\tau_{t,s}$  and the expected price  $\tau_t$ .  
 122

123 For period-level values, define the expected total mitigation cost and expected  
 124 marginal abatement cost as  $\kappa_t := \mathbb{E}_t[\kappa_{t,S}]$  and  $\kappa'_t := \mathbb{E}_t[\kappa'_{t,S}]$ . Note that be-  
 125 cause  $m_{t,s}$  is node-specific,  $\kappa'_t \neq \partial \kappa_t / \partial m$  in general. At the node level, however,  
 126  $\kappa'_{t,s}(m_{t,s}, L_{t,s}) = \partial \kappa_{t,s}(m_{t,s}, L_{t,s}) / \partial m_{t,s}$ .

127 Delaying mitigation creates a deviation from optimal choice. By not allowing for  
 128 mitigation for the first  $L$  years the world reaches the first unconstrained decision  
 129 date  $T_1 = L$  with a worse climate state: higher cumulative emissions, higher  
 130 atmospheric CO<sub>2</sub> across persistence reservoirs, and higher temperatures. In that  
 131 state, marginal damages are higher than they would have been without delay, and  
 132 the representative agent's marginal willingness to pay to avoid one ton of CO<sub>2</sub>,

<sup>4</sup>See Figure A1 for other outputs, like emissions and economic damages.

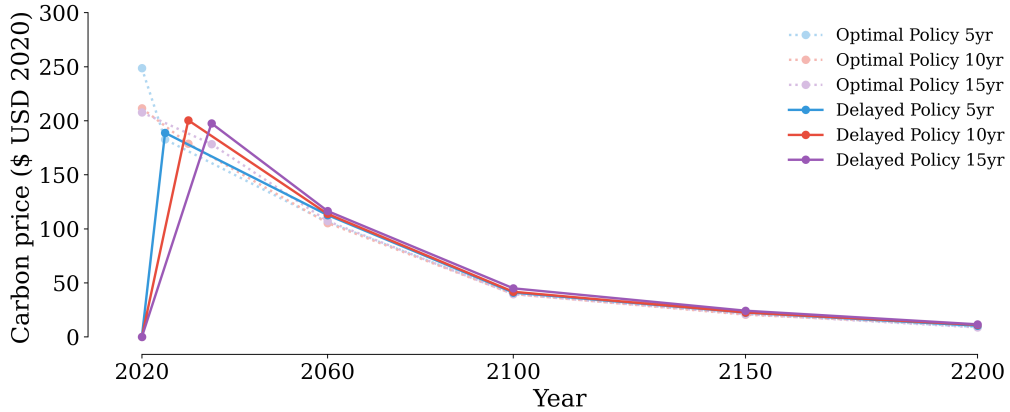


Figure 2. : Optimal CO<sub>2</sub>-price paths under delayed policy implementation.

*Note:* Six decision times are used in all runs, but the length of the first decision period is varied between 5, 10, and 15 years, while all subsequent time steps remain fixed. Each delay scenario (5 yr, 10 yr, 15 yr) is solved as an independent run. We also show a canonical baseline scenario with a decision time at the 10-year step. The resulting carbon price paths show that postponing mitigation leads to a sharp upward adjustment in the first active period, followed by convergence toward the optimal no-delay trajectory.

<sup>133</sup>  $\Phi_L(\theta_L)$ , is higher than it would have been without delay.

<sup>134</sup> Worse still, delaying mitigation also means postponing learning-by-doing. Forcing  $m_t = 0$  in the early window removes that source of endogenous cost decline (see Proposition A.1). As a result, when the world begins to act optimally at  $T_1 = L$ , it faces both a more fragile climate state and a less mature—more expensive—abatement cost curve. The representative agent’s optimal response is therefore to start the policy period with a higher expected carbon price than in the no-delay baseline, and to immediately mitigate more aggressively. This jump in the required expected entry carbon price is structural: it comes from state dependence in climate damages and from foregone technological progress, not from a particular calibration of parameters.

<sup>144</sup> Formally, under standard convexity of abatement costs and monotonicity of damages in the climate state (Appendix A.A1), the optimal expected carbon price at  $T_1 = L$  in the delayed scenario,  $\tau_L^{\text{delay}}$ , is weakly higher than the optimal expected carbon price at the same time in the no-delay baseline,  $\tau_L^{\text{base}}$ , with strict inequality whenever the no-mitigation constraint was binding. The state-

Table 1—: Delay-to-price elasticity at re-entry

$L$ (years)	Year	$\tau_L^{\text{base}}$	$\tau_L^{\text{delay}}$	$\Delta \log(\tau)$	$\eta(L)$ (%/yr)
5	2025	\$182.97	\$191.35	0.044810	0.896
10	2030	\$181.55	\$194.83	0.070607	0.706
15	2035	\$184.49	\$196.71	0.064150	0.428
					Average 0.677

<sup>149</sup> dependence logic is formalized in Proposition A.1 (Appendix A.A1).

<sup>150</sup> We summarize the expected price impact with the delay-to-price elasticity

$$(6) \quad \eta(L) := \frac{\partial \log \tau_L^{\text{delay}}}{\partial L},$$

<sup>151</sup> which is the percent increase in the required expected entry carbon price at the  
<sup>152</sup> first unconstrained decision time per additional year of forced delay. Because  
<sup>153</sup> our model is solved at discrete delay lengths only, we estimate  $\eta(L)$  by finite  
<sup>154</sup> differences using  $L \in \{5, 10, 15\}$ , i.e.,  $\eta(L) \approx (\log \tau_L^{\text{delay}} - \log \tau_L^{\text{base}})/L$ .

<sup>155</sup> Table 1 reports the resulting elasticities. For a 5-year delay, the required re-  
<sup>156</sup> entry expected price rises from \$182.97 to \$191.35, which corresponds to about an  
<sup>157</sup> 0.896% higher expected price per year of delay. For 10 and 15 years of delay, the  
<sup>158</sup> effect remains positive but declines to 0.706% and 0.428% per year, respectively.  
<sup>159</sup> Averaging across the three scenarios yields an elasticity of about 0.677% per year.  
<sup>160</sup> A simple log-linear fit of the delayed expected prices on the delay length gives a  
<sup>161</sup> smaller, global elasticity of 0.276% per year (SE: 0.000487), with a 95% confidence  
<sup>162</sup> interval of [0.181%, 0.372%]. This confirms Proposition A.1: In every scenario  
<sup>163</sup> we consider, a binding delay raises the required expected entry carbon price.  
<sup>164</sup> The elasticity is declining in  $L$ , which implies a concave delay-price relationship:  
<sup>165</sup> early years of inaction are disproportionately costly, as they push the system into  
<sup>166</sup> a higher-damage (and technically, low-learning) state, while additional years of  
<sup>167</sup> delay add to the carbon debt at a diminishing marginal rate.

<sup>168</sup> As a robustness check, we also estimate a pooled delay-to-price elasticity across

<sup>169</sup> the three scenarios by regressing the delayed re-entry expected price on the length  
<sup>170</sup> of the delay,

$$(7) \quad \log(\widehat{\tau_L^{\text{delay}}}) = \alpha + \eta^{\text{OLS}} L + \varepsilon_L,$$

<sup>171</sup> which yields  $\widehat{\log(\tau_L^{\text{delay}})} = 5.2417 + 0.0028L$ , with  $R^2 = 0.97$ . The slope coefficient  
<sup>172</sup>  $\eta^{\text{OLS}} = 0.0028$  implies that, on average across the 5-15 year range, each extra  
<sup>173</sup> year of delay raises the required expected entry carbon price by about 0.276%  
<sup>174</sup> per year. The 95% confidence interval corresponds to [0.181%, 0.372%] per year.

<sup>175</sup> **IV. Estimating deadweight losses (DWLs) of delay**

<sup>176</sup> To quantify the societal cost of delayed action, we compute the DWL associated  
<sup>177</sup> with postponing mitigation. Specifically, we determine the additional consump-  
<sup>178</sup> tion in the first period required to restore lifetime utility of the representative  
<sup>179</sup> agent to the level of the unconstrained (baseline) case. Denoting baseline utility  
<sup>180</sup> at the root as  $U_0^*$ , first-period consumption in the delayed scenario as  $c_0^D$ , and the  
<sup>181</sup> expected (certainty-equivalent) future utility as  $\text{CE}_1^D := (\mathbb{E}_0[U_1^\alpha])^{1/\alpha}$ , we define  
<sup>182</sup> the consumption-equivalent DWL  $\phi \geq 0$  implicitly by

$$(8) \quad U_0^* = \left( (1 - \beta)((1 + \phi)c_0^D)^\rho + \beta(\text{CE}_1^D)^\rho \right)^{1/\rho}.$$

<sup>183</sup> Solving for  $\phi$  yields<sup>5</sup>

$$(9) \quad \phi = \left[ \frac{(U_0^*)^\rho - \beta(\text{CE}_1^D)^\rho}{(1 - \beta)(c_0^D)^\rho} \right]^{1/\rho} - 1, \quad (\rho \neq 0).$$

<sup>184</sup> Applying this metric, we find that the DWL of delayed mitigation rises with the  
<sup>185</sup> duration of inaction (Table 2). In our main specification, enforced bans on mitiga-  
<sup>186</sup> tion force higher entry expected carbon prices at  $T_1 = L$ , which we capture with  
<sup>187</sup> the delay-to-price elasticity  $\eta(L)$ ; that higher required expected starting price

<sup>5</sup>In the case of  $\rho = 0$ , we apply the Cobb-Douglas limit as derived in Appendix A.A2

Table 2—: Social cost of delaying climate action under alternative baselines

First period length $L$ (years)	Canonical baseline		Aligned baseline		Difference (p.p.)
	DWL (%)	DWL (2020 USD tn)	DWL (%)	DWL (2020 USD tn)	
5	14.24	8.2	13.00	7.5	-1.24
10	21.82	12.6	21.87	12.7	+0.05
15	32.21	18.7	33.10	19.1	+0.89

*Note:* Deadweight loss (DWL) represents the consumption-equivalent compensation required for lifetime utility in the delayed-mitigation scenario to equal that in the corresponding baseline. The canonical baseline fixes the first decision period at 10 years across all runs to enable direct DWL comparisons. The aligned baseline matches each delay scenario to an unconstrained run with the same decision timeline (e.g., 5-year delay vs. 5-year baseline). The minor difference for the 10-year scenario reflects stochastic draws in the model’s Monte Carlo simulations. Dollar values are in trillions of 2020 USD.

<sup>188</sup> translates directly into a larger consumption-equivalent DWL  $\phi$ . In our main  
<sup>189</sup> specification, banning mitigation for five years, ten years, and fifteen years pro-  
<sup>190</sup>duces a DWL of delay of roughly 14%, 22%, and 32% of first-period consumption,  
<sup>191</sup> respectively. In monetary terms, these correspond to about \$8.3tn, \$12.8tn, and  
<sup>192</sup>\$18.8tn in one-time global compensation at the start of the policy window. Each  
<sup>193</sup>additional year of delay raises the DWL by about \$1.05 trillion per year over the  
<sup>194</sup>5–15 year range, i.e., roughly 1.8 percentage points of first-period consumption  
<sup>195</sup>per year. A simple log-log fit implies  $\phi(L) \propto L^{0.73}$ , indicating sub-linear scaling  
<sup>196</sup>and modestly declining marginal losses as the delay lengthens.

<sup>197</sup> These DWLs increase with delay length, but not linearly. Longer bans on  
<sup>198</sup>mitigation give the representative agent at the next decision time a more polluted  
<sup>199</sup>atmosphere and therefore require a higher expected starting carbon price at  $T_1 =$   
<sup>200</sup> $L$  under our standard assumptions. The agent then responds by catching up:  
<sup>201</sup>once mitigation is finally allowed, the optimal policy sharply raises the expected  
<sup>202</sup>carbon price at  $T_1 = L$  relative to the no-delay baseline and moves immediately  
<sup>203</sup>to very aggressive abatement. This catch-up behavior is economically painful in  
<sup>204</sup>the short run, which shows up in  $\phi(L)$ , but it stabilizes the long run by limiting  
<sup>205</sup>further deterioration of the climate-economy state. Numerically, in our baseline

206 calibration  $\phi(L)$  rises quickly between 0 and 10 years of delay and continues to  
207 rise thereafter, though at a slower rate (Table 2). In our benchmark runs, then,  
208 the exogenously induced delay has a clearly measurable cost: for the 5-15 year  
209 range we study, every additional year without mitigation forces the social planner  
210 to start the policy period with an expected carbon price between about 0.4 and  
211 0.9 percent higher than it otherwise would have been, with an average of 0.7  
212 percent. The regression-based estimate is smaller because it smooths across the  
213 three scenarios, but it preserves the sign and the basic message: delay makes the  
214 first feasible expected carbon price higher.

215 Figure 3 examines the consequences of relaxing the stringency of the first-period  
216 policy constraint by imposing an upper bound  $m(t) \leq p$  on the mitigation rate  
217 over the initial interval  $t \in [0, L]$ , where  $p \in [0, 1]$  denotes the maximum share  
218 of baseline emissions that may be abated. For caps close to the unconstrained  
219 solution, the DWL increases approximately quadratically in the cap's tightness,  
220 with the level of the loss rising in the duration of the delay  $L$ .

221 This quadratic relationship provides a simple heuristic for why even limited  
222 early mitigation recovers a disproportionate fraction of welfare, and why DWL  
223 converges rapidly to zero as  $p$  approaches the smallest nonbinding cap (and the  
224 constraint ceases to bind). Conversely, the marginal welfare gain from relaxing  
225 the constraint is decreasing in  $p$ .

## 226 **V. Evaluating parameter importance**

227 Understanding why delay is so costly requires unpacking which structural prim-  
228 itives make the carbon-debt difference  $\tau_L^{\text{delay}} - \tau_L^{\text{base}}$  and its elasticity as per Equa-  
229 tion (6) large, and therefore drive the DWL penalty  $\phi$ . Figure 4 offers a first look,  
230 plotting the DWL of delay against four structural drivers: EIS, PRTP, exogenous  
231 technological change, and endogenous learning. Lines show within-delay OLS fits  
232 of the expected DWL on the parameter value. The fitted Gaussian curves show  
233 the distribution of  $\phi(L)$  for the different delay lengths given our parameter space.

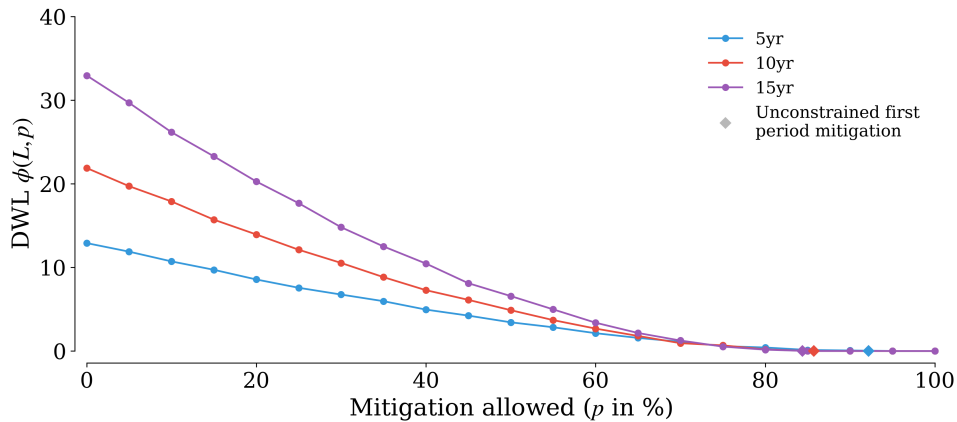


Figure 3. : DWL as a function of allowed partial mitigation  $p$  in the first period.

*Note:* Policies are compared under the aligned baseline in the main specification (see Appendix A.A1). Small variation in smoothness are due to the stochastic nature of the model.

234 The central result is that impatience dominates. When societies heavily discount  
 235 the future, no amount of technological progress or learning can offset the welfare  
 236 lost from postponing mitigation.

237 Parameter sensitivities in Table 3 show which economic mechanisms drive the  
 238 DWL of delaying climate action in a multivariate regression, i.e., they show partial  
 239 OLS effects within our parameter grid. We estimate these effects over a broad  
 240 random draw of the model’s structural parameters, each sampled independently  
 241 from its prior probability distribution. This approach ensures that coefficients  
 242 capture partial effects across the full range of plausible economic and technological  
 243 states. Each parameter thus maps a structural assumption into an economic  
 244 intuition about risk, time, and technology.

245 Higher risk aversion (RA) raises the shadow value of insurance against uncertain  
 246 climate damages. A one-point increase in  $\gamma$  raises the DWL by roughly 0.25  
 247 percentage points, or about \$147 billion. This result is highly significant. Agents  
 248 who are risk-averse value early mitigation more strongly as protection against  
 249 catastrophic tail outcomes. Nonetheless, RA across states of nature matters less  
 250 than aversion across time (see EIS): what dominates is not which climate future

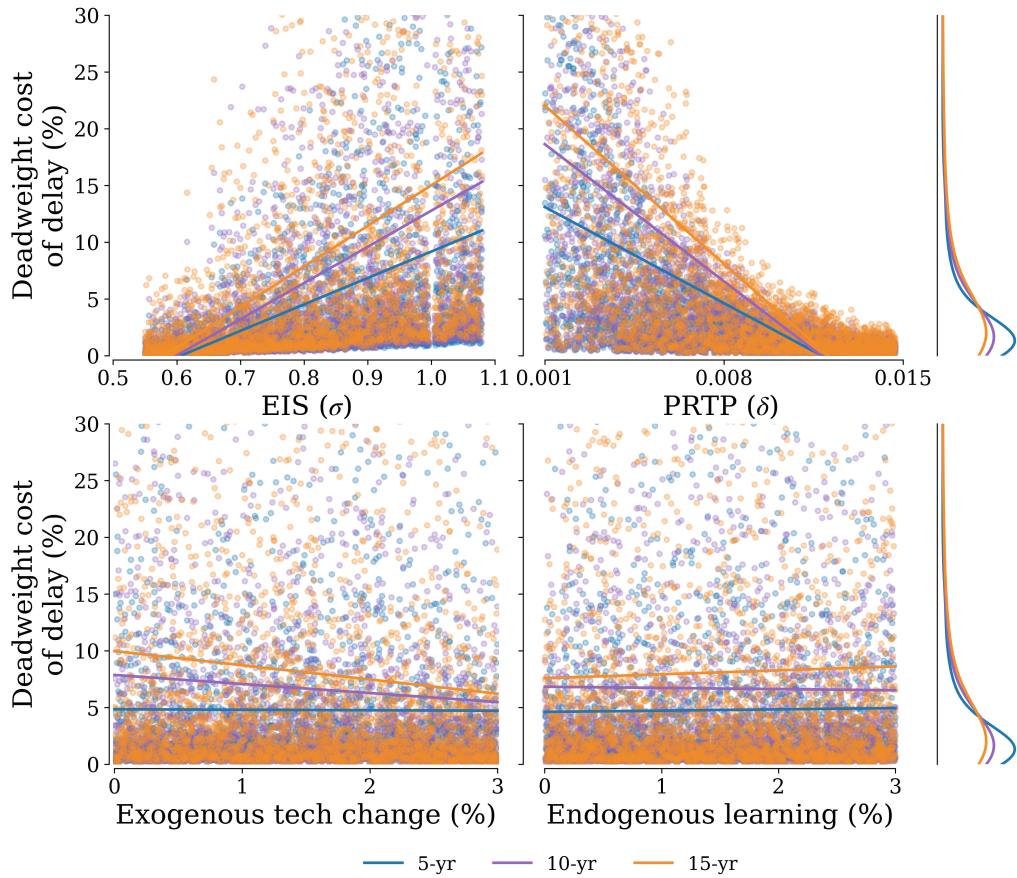


Figure 4. : Variance decomposition of deadweight losses (DWLs) by structural parameters.

*Note:* The figure truncates the vertical axis at 30% to improve visibility. This range contains approximately 95% of observations.

251 occurs but how long society waits to act.

252 The EIS is the single strongest behavioral determinant of delay costs. A 0.1  
 253 increase in  $\sigma$  (within the sampled range of 0.55-1.1) raises the DWL by about  
 254 5%, or \$3 trillion ( $p < 0.001$ ). In the unconstrained baseline, such a society is  
 255 willing to sacrifice some near-term consumption (via costly early mitigation) in  
 256 exchange for much lower climate damages later. A binding delay prevents that  
 257 optimal intertemporal trade, so the DWL  $\phi(L)$  from delay is larger when  $\sigma$  is  
 258 high.

Table 3—: Regression results: determinants of deadweight loss (DWL) and mitigation delay outcomes

	(1)	(2)	(3)
Const	-0.0457** (0.0199)	-10.5381 (8.3528)	-6301.7279 (4994.9064)
RA ( $\gamma$ )	0.0046*** (0.0002)	0.2454*** (0.0847)	146.7690*** (50.6514)
EIS ( $\sigma$ )	0.4767*** (0.0057)	49.7372*** (2.5267)	29742.5249*** (1510.9441)
Tech. change (exog.)	-1.4735*** (0.0935)	-73.5360* (38.5723)	-43974.0590* (23066.0244)
Tech. learning (endo.)	0.8882*** (0.0883)	63.7416* (34.3644)	38117.0615* (20549.6858)
PRTP ( $\delta$ )	-23.5410*** (0.2509)	-2556.3668*** (111.3807)	-1528691.37*** (66604.9448)
log(Backstop premium)	-0.0009 (0.0020)	-0.6235 (0.8472)	-372.8457 (506.6172)
Cons. growth	-3.5662*** (0.1814)	-57.4224 (77.6601)	-34338.2212 (46440.2569)
Delay 10	0.0469*** (0.0015)	3.4608*** (0.3973)	2069.5203*** (237.5642)
Delay 15	0.1088*** (0.0021)	8.5027*** (0.7598)	5084.5728*** (454.3852)
R <sup>2</sup>	0.7639	0.2034	0.2034
Adj. R <sup>2</sup>	0.7636	0.2026	0.2026
N	8830	8830	8830

*Note:* Results from an OLS regression with time fixed effects (Delay 10 and 15). Heteroskedasticity-robust standard errors in parentheses. All specifications include the same nine regressors. Delay 10 and Delay 15 are indicator variables for the different delay periods and reference delay 5. The dependent variable in column (1) is the utility loss (in %) from delaying optimal climate policy. Column (2) uses the consumption-equivalent DWL ( $\phi(L)$  in %), and column (3) uses the absolute DWL in billions of 2020 USD.

\*\*\*  $p < 0.01$ , \*\*  $p < 0.05$ , \*  $p < 0.1$ .

259 With a negative coefficient significant at the 10% level, faster exogenous tech-  
 260 nological change cushions the economy against delay. A one percentage-point  
 261 increase in the exogenous rate of technological change reduces DWL by roughly  
 262 0.7%, or about \$440 billion. Independent innovation lowers future abatement  
 263 costs and partially offsets delay. When technology improves independently of

264 early action, postponement hurts less because future abatement is cheaper. Con-  
265 versely, technological stagnation amplifies the cost of delay.

266 Endogenous technological learning has a positive coefficient that is significant  
267 at the 10% level with similar magnitude to exogenous change. A one percentage-  
268 point increase in learning intensity raises DWL by about 0.6%, or \$380 billion.  
269 The mechanism is path dependence: delaying mitigation slows learning-by-doing,  
270 delaying cost reductions and locking in higher future abatement costs. Inaction  
271 today undermines tomorrow's productivity gains.

272 PRTP ( $\delta$ ) has a large and statistically significant effect. The coefficient im-  
273 plies that raising  $\delta$  by 1 percentage point lowers DWL by roughly 25.6 percentage  
274 points, or \$ 15.3 trillion. More impatient societies (higher  $\delta$ , lower  $\beta$ ) care rela-  
275 tively less about distant future damages. In our regressions, this shows up as a  
276 lower measured DWL from delay. Conversely, patient societies (low  $\delta$ ) view delay  
277 as extremely expensive. This confirms that how we value time, not technology or  
278 static risk, is a first-order driver of the DWL variation across scenarios.

279 The backstop premium, that is, the long-run cost ceiling for zero-carbon tech-  
280 nology, is statistically insignificant and economically negligible. A 1% change in  
281 the backstop price shifts DWL by less than 0.01%, or about \$0.4 billion. In the  
282 model, this parameter adds a surcharge to the marginal cost of over-mitigation,  
283 that is, for mitigation levels above 100%, corresponding to net carbon removal.  
284 This captures the real-world cost gap between eliminating emissions and achieving  
285 net-negative emissions through technologies such as direct air capture. Because  
286 optimal policy paths in our delay experiments rarely enter the over-mitigation  
287 regime, the DWL effects of the premium remain small.

288 Consumption growth enters negatively. A 1-percentage-point faster consump-  
289 tion rate reduces the DWL by about 0.6%, or \$340 billion. Even though it is  
290 not significant, the sign aligns with the theoretical expectation that faster growth  
291 decreases the DWL of delay.

292 Both delay length indicator variables are positive and highly significant. Ex-

<sup>293</sup> tending the first decision period from 5 to 10 years raises the DWL by about  
<sup>294</sup> 3.5%, or \$2.1 trillion; extending to 15 years increases them by roughly 8.5%, or  
<sup>295</sup> \$5.1 trillion. The rise is steep but concave, consistent with the model's adaptive  
<sup>296</sup> catch-up dynamics: once mitigation begins, expected carbon prices jump sharply,  
<sup>297</sup> partially—but never fully—recovering lost welfare.

<sup>298</sup> Taken together, our analysis shows that the economics of delay is fundamentally  
<sup>299</sup> about time preference and intertemporal trade-offs: Impatience and substitution,  
<sup>300</sup> not technology or risk, explain most of the DWL of inaction, underscoring that  
<sup>301</sup> the true price of delay is paid in lost time. Optimal carbon price paths and DWL  
<sup>302</sup> results under different sets of parameter assumption are in Figures A3 and A4.

## REFERENCES

304 **Ackerman, Frank, Elizabeth A Stanton, and Ramón Bueno.** 2013.  
305 “Epstein–Zin utility in DICE: Is risk aversion irrelevant to climate policy?” *En-*  
306 *vironmental and Resource Economics*, 56(1): 73–84.

307 **Bauer, Adam Michael, Cristian Proistosescu, and Gernot Wagner.** 2024.  
308 “Carbon Dioxide as a Risky Asset.” *Climatic Change*, 177(5): 72.

309 **Bertram, Christoph, Elina Brutschin, Laurent Drouet, Gunnar Lud-**  
310 **erer, Bas van Ruijven, Lara Aleluia Reis, Luiz Bernardo Baptista,**  
311 **Harmen-Sytze de Boer, Ryna Cui, Vassilis Daioglou, et al.** 2024. “Fea-  
312 sibility of peak temperature targets in light of institutional constraints.” *Nature*  
313 *Climate Change*, 14(9): 954–960.

314 **Bilal, Adrien, and Diego R Käenzig.** 2025. “The macroeconomic impact of  
315 climate change: Global vs. local temperature.” National Bureau of Economic  
316 Research.

317 **Burke, Marshall, Solomon M. Hsiang, and Edward Miguel.** 2015. “Global  
318 non-linear effect of temperature on economic production.” *Nature*, 527(7577): 235–  
319 239.

320 **Burke, Marshall, W. Matthew Davis, and Noah S. Diffenbaugh.** 2018.  
321 “Large potential reduction in economic damages under UN mitigation targets.”  
322 *Nature*, 557(7706): 549–553.

323 **Clausing, Kimberly A., Christopher R. Knittel, and Catherine Wol-**  
324 **fram.** 2025. “Who Bears the Burden of Climate Inaction?”

325 **Daniel, Kent D., Robert B. Litterman, and Gernot Wagner.** 2019.  
326 “Declining CO<sub>2</sub> price paths.” *Proceedings of the National Academy of Sciences*,  
327 116(42): 20886–20891.

328 **Dechezleprêtre, Antoine, Adrien Fabre, Tobias Kruse, Blueberry**  
329 **Planterose, Ana Sanchez Chico, and Stefanie Stantcheva.** 2025. “Fight-  
330 ing climate change: International attitudes toward climate policies.” *American*  
331 *Economic Review*, 115(4): 1258–1300.

332 **Dietz, Simon, James Rising, Tobias Stoerk, and Gernot Wagner.** 2021.  
333 “Economic impacts of tipping points in the climate system.” *Proceedings of the*  
334 *National Academy of Sciences*, 118(34): e2103081118.

335 **Epstein, Larry G, and Stanley E Zin.** 1989. “Substitution, Risk Aversion,  
336 and the Temporal Behavior of Consumption and Asset Returns: A Theoretical  
337 Framework.” *Econometrica: Journal of the Econometric Society*, 937–969.

338 **Epstein, Larry G, and Stanley E Zin.** 1991. “Substitution, risk aversion, and  
339 the temporal behavior of consumption and asset returns: An empirical analysis.”  
340 *Journal of political Economy*, 99(2): 263–286.

341 **Howard, Peter H., and Thomas Sterner.** 2017. “Few and Not So Far Be-  
342 tween: A Meta-analysis of Climate Damage Estimates.” *Environmental and Re-*  
343 *source Economics*, 68(1): 197–225.

344 **Intergovernmental Panel on Climate Change (IPCC).** 2023. “Climate  
345 Change 2023: Synthesis Report. Contribution of Working Groups I, II and III to  
346 the Sixth Assessment Report of the Intergovernmental Panel on Climate Change.”  
347 Intergovernmental Panel on Climate Change (IPCC), Geneva, Switzerland.

348 **Joos, F., R. Roth, J. S. Fuglestvedt, G. P. Peters, I. G. Enting, W. von**  
349 **Bloh, V. Brovkin, E. J. Burke, M. Eby, N. R. Edwards, T. Friedrich,**  
350 **T. L. Frölicher, P. R. Halloran, P. B. Holden, C. Jones, T. Kleinen,**  
351 **F. T. Mackenzie, K. Matsumoto, M. Meinshausen, G.-K. Plattner, A.**  
352 **Reisinger, J. Segschneider, G. Shaffer, M. Steinacher, K. Strassmann,**  
353 **K. Tanaka, A. Timmermann, and A. J. Weaver.** 2013. “Carbon dioxide and

354 climate impulse response functions for the computation of greenhouse gas metrics:  
355 a multi-model analysis.” *Atmospheric Chemistry and Physics*, 13(5): 2793–2825.

356 **Lemoine, Derek, and Christian Traeger.** 2014. “Watch your step: optimal  
357 policy in a tipping climate.” *American Economic Journal: Economic Policy*,  
358 6(1): 137–166.

359 **Meckling, Jonas.** 2025. “The geoeconomic turn in decarbonization.” *Nature*,  
360 645(8082): 869–876.

361 **Meckling, Jonas, Thomas Sterner, and Gernot Wagner.** 2017. “Policy  
362 sequencing toward decarbonization.” *Nature Energy*, 2(12): 918–922.

363 **Mildenberger, Matto.** 2020. *Carbon captured: How business and labor control  
364 climate politics*. MIT Press.

365 **Mildenberger, Matto, and Dustin Tingley.** 2019. “Beliefs about climate be-  
366 liefs: the importance of second-order opinions for climate politics.” *British Journal  
367 of Political Science*, 49(4): 1279–1307.

368 **Moore, Frances C, Moritz A Drupp, James Rising, Simon Dietz, Ivan  
369 Rudik, and Gernot Wagner.** 2024. “Synthesis of evidence yields high social  
370 cost of carbon due to structural model variation and uncertainties.” *Proceedings  
371 of the National Academy of Sciences*, 121(52): e2410733121.

372 **Oreskes, Naomi, and Erik M Conway.** 2011. *Merchants of doubt: How a  
373 handful of scientists obscured the truth on issues from tobacco smoke to global  
374 warming*. Bloomsbury Publishing USA.

375 **Rose, Steven K., Delavane B. Diaz, and Geoffrey J. Blanford.** 2017. “Un-  
376 derstanding the Social Cost of Carbon: A Model Diagnostic and Inter-comparison  
377 Study.” *Climate Change Economics*, 8(02): 1750009.

378 **Stechemesser, Annika, Nicolas Koch, Ebba Mark, Elina Dilger, Patrick  
379 Klösel, Laura Menicacci, Daniel Nachtigall, Felix Pretis, Nolan Ritter,**

<sup>380</sup> **Moritz Schwarz, et al.** 2024. “Climate policies that achieved major emission  
<sup>381</sup> reductions: Global evidence from two decades.” *Science*, 385(6711): 884–892.

<sup>382</sup> **Traeger, Christian P.** 2014. “Why uncertainty matters: discounting under  
<sup>383</sup> intertemporal risk aversion and ambiguity.” *Economic Theory*, 56(3): 627–664.

<sup>384</sup> **Wagner, Gernot, and Richard J Zeckhauser.** 2012. “Climate policy: hard  
<sup>385</sup> problem, soft thinking.” *Climatic change*, 110(3): 507–521.

*A1. Model and dynamics*

388 This section formally describes the model setup and proves Proposition A.1.  
 389 Decisions occur on a finite set of times  $T_0, T_1, \dots, T_N$ , measured in calendar years  
 390 (e.g.,  $T_0 = 2020, T_1 \in \{2025, 2030, 2035\}$ , etc.). At each decision time  $T_t$  and  
 391 node, the social planner (our representative agent) chooses the mitigation rate  
 392  $m_t \in [0, \bar{m}]$  that applies over the entire subsequent interval  $[T_t, T_{t+1})$ . Values  
 393  $m_t > 1$  are net removal of CO<sub>2</sub> (direct air capture and related negative-emissions  
 394 technologies) at a backstop premium. In our benchmark calibration,  $\bar{m} = 1.5$  and  
 395 the backstop premium is \$10,000.

396 Following Daniel, Litterman and Wagner (2019), we embed the planner in a non-  
 397 recombining binomial tree in which each node inherits a current fragility state that  
 398 indexes how severe climate damages have turned out so far. The high-fragility  
 399 branches correspond to high realized damages (or bad climate/economic states),  
 400 and the low-fragility branch to more benign outcomes. Uncertainty therefore  
 401 resolves gradually along the tree rather than all at once. At each node, the agent  
 402 re-optimizes given the currently realized state.

403 This structure matters for two reasons. First, it makes the problem explic-  
 404 itly stochastic as future consumption, temperature, and damages differ across  
 405 branches. Second, it allows us to separate aversion to risk across time from  
 406 aversion to risk across states of nature. The same structure also lets us impose  
 407 politically relevant constraints on early climate policy: we can constrain the agent  
 408 not to mitigate for an initial window and then ask how the system behaves once  
 409 the constraint is lifted.

410 We analyze delays in mitigation by imposing an exogenous no-mitigation period  
 411 of length  $L$  years. Formally, for a given  $L \in \{5, 10, 15\}$ , we impose  $m_t = 0$  for all  
 412 decision times  $T_t < L$ , and relax this constraint for  $T_t \geq L$ .<sup>6</sup> We compare each

<sup>6</sup>In our standard calibration, this corresponds to constraining  $T_0$  only.

413 scenario to a common unconstrained baseline with a node at  $T_t = 10$  in which  
 414 the planner is free to choose  $m_t$  at all decision times.

415 Preferences follow a standard Epstein-Zin recursive specification as in Equa-  
 416 tion (1) with terminal utility given by Equation (2). For our main specification,  
 417 parameter values are as follows:  $\text{PRTP}(\delta) = 0.002$ ;  $\text{EIS}(\sigma) = 0.833$ ;  $\text{RA}(\gamma) = 10$ ;  
 418 consumption growth p.a. = 0.02; exog. tech change = 0.015; endo. tech learning =  
 419 0; baseline emissions = SSP2; backstop premium = 10 000.

420 EMISSIONS, CLIMATE DYNAMICS, COSTS, AND DAMAGES

421 For expositional clarity, throughout this subsection we fix an arbitrary realiza-  
 422 tion (i.e., path) of uncertainty and suppress state indices; all objects  $(m_t, \theta_t, L_t, \kappa_t, \Phi_t, \tau_t)$  are  
 423 thus defined along a single path in our binomial tree.

424 Let  $E_t > 0$  denote the baseline (business-as-usual) CO<sub>2</sub> emissions over the  
 425 interval  $[T_t, T_{t+1})$ , based on a reference socioeconomic pathway (e.g., SSP2). The  
 426 planner can abate a fraction  $m_t \in [0, \bar{m}]$  of those baseline emissions, so realized  
 427 emissions over that interval are

$$(A1) \quad e_t = (1 - m_t)E_t.$$

428 The climate state at time  $T_t$  is characterized by two key variables: atmospheric  
 429 CO<sub>2</sub> concentration  $C_t$  (in ppm) and temperature anomaly  $\theta_t$  (in °C above prein-  
 430 dustrial).

431 Atmospheric CO<sub>2</sub> concentration  $C_t$  evolves as the convolution of past emissions  
 432 with the impulse response function (IRF) of the carbon cycle, following Joos et al.  
 433 (2013):

$$(A2) \quad C_t = C_0 + \chi \int_0^t \Psi(t-s)e_s ds, \quad \text{where } \Psi(s) = a_0 + \sum_{i=1}^3 a_i \exp(-s/b_i),$$

434 with  $\chi = 1/7.8 = 0.128$  ppm/GtCO<sub>2</sub> and coefficients  $a_0 = 0.2173$ ,  $a_1 = 0.2240$ ,

<sup>435</sup>  $a_2 = 0.2824$ ,  $a_3 = 0.2763$ , and time constants  $b_1 = 394.4$ ,  $b_2 = 36.54$ ,  $b_3 = 4.304$   
<sup>436</sup> years. All  $a_i, b_i > 0$ , so concentrations are strictly increasing in cumulative  
<sup>437</sup> emissions. These parameters capture the multiple carbon-cycle reservoirs (at-  
<sup>438</sup>mosphere, mixed-layer ocean, deep ocean, biosphere) and the long-lived airborne  
<sup>439</sup>fraction  $a_0$ .

<sup>440</sup> The global mean surface temperature anomaly  $\theta_t$  is linked to cumulative emis-  
<sup>441</sup> sions through the Transient Climate Response to Cumulative Emissions (TCRE)  
<sup>442</sup> framework following AR6:

$$(A3) \quad \theta_t = \lambda_{\text{eff}} \int_0^t e_u du, \quad \lambda_{\text{eff}} := \frac{\lambda}{1 - f_{\text{nc}}}.$$

<sup>443</sup> Here  $e_u$  denotes CO<sub>2</sub> emissions at time  $u$  measured in thousand gigatonnes of  
<sup>444</sup> CO<sub>2</sub> per year (TtCO<sub>2</sub>/yr), so that  $\int_0^t e_u du$  is cumulative emissions in thousands  
<sup>445</sup> GtCO<sub>2</sub>. The parameter  $\lambda > 0$  (in K per 1000 GtCO<sub>2</sub>) is the TCRE for CO<sub>2</sub>-  
<sup>446</sup> only warming, while  $f_{\text{nc}} \in (0, 1)$  scales in the contribution from non-CO<sub>2</sub> forcing.  
<sup>447</sup> Following Bauer, Proistosescu and Wagner (2024), we take the effective TCRE to  
<sup>448</sup> be  $\lambda_{\text{eff}} \sim \mathcal{N}(0.52, 0.21^2)$  K per TtCO<sub>2</sub>.

<sup>449</sup> This formulation implies three key properties for our analytical results:

- <sup>450</sup> (i)  $C_t$  and  $\theta_t$  are strictly increasing in the emissions path  $\{e_s\}_{s \leq t}$  because  
<sup>451</sup>  $\Psi(\zeta) \geq 0$  and  $\lambda_{\text{eff}} > 0$ .
- <sup>452</sup> (ii) The multi-timescale IRF ensures that past emissions affect concentrations  
<sup>453</sup> far into the future, with fraction  $a_0$  remaining indefinitely.
- <sup>454</sup> (iii) High emissions in  $[T_i, T_{i+1})$  permanently elevate both  $C_t$  and  $\theta_t$  for all sub-  
<sup>455</sup> sequent times.

<sup>456</sup> Based on Burke, Davis and Diffenbaugh (2018); Rose, Diaz and Blanford (2017);  
<sup>457</sup> Howard and Sterner (2017); Dietz et al. (2021), damages are represented as the  
<sup>458</sup> sum of an aggregate temperature-based loss component and an additional com-

459 ponent from climate tipping points:

$$(A4) \quad d_t = D^{(k)}(\theta_t) + d_{tp}(\theta_t), \quad D^{(k)}(\theta_t) = \delta_1^{(k)}\theta_t + \delta_2^{(k)}\theta_t^2$$

460 where  $k \in \{\text{statistical, structural, meta}\}$  indexes the aggregate damage family,  
 461 and  $d_{tp}(\theta_t)$  captures the expected effect of climate tipping events. The coefficients  
 462  $(\delta_1^{(k)}, \delta_2^{(k)})$  were calibrated by (Bauer, Proistosescu and Wagner, 2024) from the  
 463 respective sources and may vary across periods<sup>7</sup>, but for any fixed  $t$ , each  $D^{(k)}$  is  
 464 quadratic in  $\theta_t$  and increasing on the temperature range we study (0-6°C).

465 The structural IAM function (Rose, Diaz and Blanford, 2017) and the meta-  
 466 analytic function (Howard and Sterner, 2017) are convex ( $\delta_{2,t}^{(\cdot)} > 0$ ) over our  
 467 calibration. The statistical function (Burke, Hsiang and Miguel, 2015) is convex  
 468 through mid-century and becomes mildly concave in late-century ( $\delta_{2,t}^{(\text{stat})} < 0$  for  $t$   
 469 after 2100) but remains increasing on the relevant temperature range. The tipping  
 470 component  $d_{tp}(\theta_t)$  is also quadratic with positive curvature (Dietz et al., 2021),  
 471 so it raises marginal damages at higher temperatures. To not rely too heavily  
 472 on single estimates, our main specification averages across the three aggregate  
 473 families with equal probability and adds the tipping component in every draw.  
 474 Hence, we define the model-averaged damages at time  $t$  as

$$(A5) \quad \bar{D}(\theta_t) := \mathbb{E}_k \left[ D^{(k)}(\theta_t) + d_{tp}(\theta_t) \right] \quad \forall k,$$

475 where the expectation is over the three aggregate families with equal weights. In  
 476 our main specification, this means  $\bar{D}(\theta_t)$  is twice continuously differentiable and  
 477 satisfies

$$(A6) \quad \frac{d\bar{D}(\theta_t)}{d\theta_t} > 0 \quad \text{and} \quad \frac{d^2\bar{D}(\theta_t)}{d\theta_t^2} \geq 0$$

<sup>7</sup>The statistical specification from (Burke, Hsiang and Miguel, 2015), for example, uses distinct mid- and end-century calibration.

478 for temperatures between 0 and 6 °C.

479 The period- $t$  marginal abatement cost curve (MACC) follows the exponential  
 480 form and is calibrated to IPCC AR6 Working Group III data (Intergovernmental  
 481 Panel on Climate Change , IPCC), consistent with Bauer, Proistosescu and  
 482 Wagner (2024). For a mitigation rate  $m_t \in [0, \bar{m}]$  and technology and learning  
 483 state  $L_t$ , which captures both exogenous and endogenous technological progress,  
 484 we specify

$$(A7) \quad \tau_t(m_t, L_t) = \begin{cases} L_t \tau_0 (e^{\xi m_t} - 1), & 0 \leq m_t \leq 1, \\ L_t (\tau_0 + \tau^{\text{prem}}) (e^{\xi m_t} - 1), & m_t > 1, \end{cases}$$

485 where  $\tau_0 > 0$  and  $\xi > 0$  are level and curvature parameters, and  $\tau^{\text{prem}} > 0$  is a  
 486 backstop premium representing the additional cost of net-negative emissions (e.g.,  
 487 direct air capture). The corresponding total mitigation cost function is obtained  
 488 by integrating the marginal cost curve for  $m_t \leq 1$ ,

$$(A8) \quad \kappa_t(m_t, L_t) = L_t \tau_0 \left( \frac{e^{\xi m_t} - 1}{\xi} - m_t \right), \quad (0 \leq m_t \leq 1),$$

489 and analogously with  $\tau_0 + \tau^{\text{prem}}$  for  $m_t > 1$ .<sup>8</sup> On each regime  $m_t \in [0, 1]$  and  
 490  $m_t > 1$ , the function  $\kappa_t(\cdot, \cdot)$  is twice continuously differentiable, strictly increasing  
 491 and convex in  $m_t$ , and weakly increasing in the learning factor  $L_t$ . Higher  $L_t$   
 492 indicates less technological progress and therefore higher costs, while lower  $L_t$   
 493 reflects learning-by-doing and innovation that shift the MACC downward.

494 The learning factor  $L_t$  evolves according to cumulative mitigation experience  
 495 and exogenous technological improvement. Hence,

$$(A9) \quad L_t = (1 - \psi_0 - \psi_1 X_t)^{(Y_t - Y_{\text{ref}})},$$

496 where  $Y_t$  is the calendar year at decision time  $T_t$ ,  $Y_{\text{ref}}$  is the reference year used

<sup>8</sup>Note that this creates a level jump at  $m_t = 1$ .

497 for calibration (2030 in our baseline), and parameters  $\psi_0 \geq 0$  and  $\psi_1 \geq 0$  capture  
 498 exogenous and endogenous technological progress, respectively. The term  $X_t$   
 499 represents the weighted average mitigation up to time  $t$ ,

$$(A10) \quad X_t := \frac{\int_0^t m(\zeta)E(\zeta)d\zeta}{\int_0^t E(\zeta)d\zeta},$$

500 so that stronger cumulative mitigation or faster exogenous innovation lowers  $L_t$   
 501 and thereby reduces future abatement costs.

502 Let  $y_t$  be gross resources available for consumption at time  $T_t$ . Actual con-  
 503 sumption is then determined by

$$(A11) \quad c_t = y_t - \kappa_t(m_t, L_t) - d_t(\theta_t).$$

504 Delay thus reduces consumption through a more deteriorated climate state caus-  
 505 ing higher damages, and slower cost decline raising mitigation costs.

506 OPTIMAL EXPECTED CARBON PRICES

507 To compare policies at a given decision time  $t$ , we now take expectations across  
 508 nodes, as in the main text (see Equation (3)).

509 *Proposition A.1.* (Delay raises the expected entry carbon price) *Assume baseline*  
 510 *emissions are strictly positive in all periods prior to  $T_1$ , i.e.,  $E_t > 0$  for all*  
 511  *$T_t < T_1$ . Suppose:*

- 512 (i) *The delay constraint is binding in the baseline period, i.e., there exists  $t < T_1$*   
 513 *with  $m_t^{base} > 0$ , while in the delayed scenario  $m_t^{delay} = 0$  for all  $T_t < T_1$ ;*
- 514 (ii) *The carbon-cycle and TCRE mappings in (A2)–(A3) satisfy  $\Psi(\zeta) \geq 0$  and*  
 515  *$\lambda_{eff} > 0$ , so climate dynamics are monotone;*
- 516 (iii) *Model-averaged damages are increasing and weakly convex:  $\bar{D}'(\theta) > 0$  and*  
 517  *$\bar{D}''(\theta) \geq 0$  (cf. (A5));*

518 (iv) The optimal  $m_{T_1}$  is interior in both the base and delay scenarios.

519 Then, for every node  $s \in \mathcal{S}_{T_1}$ ,  $\tau_{T_1,s}^{\text{delay}} \geq \tau_{T_1,s}^{\text{base}}$ , and therefore, taking expectations  
520 across nodes,

$$(A12) \quad \tau_1^{\text{delay}} \geq \tau_1^{\text{base}},$$

521 with strict inequality whenever  $\theta_{T_1,s}^{\text{delay}} > \theta_{T_1,s}^{\text{base}}$  on a set of nodes with positive probability  
522 (equivalently, when  $\mathbb{E}_1[\theta_{1,S}^{\text{delay}}] > \mathbb{E}_1[\theta_{1,S}^{\text{base}}]$ ).

523 *Proof.* Fix an arbitrary node  $s \in \mathcal{S}_{T_1}$  and consider the unique history (path) leading  
524 to  $s$  under the baseline and delayed scenarios. By construction,  $m_t^{\text{delay}} = 0$  for  
525 all  $T_t < T_1$ , while by (i) there exists some  $t < T_1$  with  $m_t^{\text{base}} > 0$ . From (A1), for  
526 at least one such  $t$  we have  $e_t^{\text{delay}} = (1 - 0)E_t = E_t > (1 - m_t^{\text{base}})E_t = e_t^{\text{base}}$ . Hence  
527 cumulative emissions up to  $T_1$  are (weakly) higher along the delayed path. By (ii)  
528 and the monotonicity of the carbon-cycle IRF and TCRE mappings (A2)–(A3),  
529 higher past emissions imply a (weakly) worse climate state at  $T_1$ :  $C_{T_1,s}^{\text{delay}} \geq C_{T_1,s}^{\text{base}}$   
530 and  $\theta_{T_1,s}^{\text{delay}} \geq \theta_{T_1,s}^{\text{base}}$ , with strict inequality if baseline mitigation was positive on  
531 a nonzero set. By (iii), marginal damages are increasing in temperature, so  
532  $\Phi_{T_1,s}(\theta_{T_1,s}^{\text{delay}}) \geq \Phi_{T_1,s}(\theta_{T_1,s}^{\text{base}})$ , strictly when  $\theta_{T_1,s}^{\text{delay}} > \theta_{T_1,s}^{\text{base}}$ . Under the interior first-  
533 order condition at node  $(T_1, s)$ ,  $\tau_{T_1,s}^{\text{delay}} = \Phi_{T_1,s}(\theta_{T_1,s}^{\text{delay}})$  and  $\tau_{T_1,s}^{\text{base}} = \Phi_{T_1,s}(\theta_{T_1,s}^{\text{base}})$ ,  
534 which implies the path-wise inequality  $\tau_{T_1,s}^{\text{delay}} \geq \tau_{T_1,s}^{\text{base}}$ . Taking expectations across  
535 nodes yields  $\tau_1^{\text{delay}} = \mathbb{E}_{T_1}[\tau_{T_1,S}^{\text{delay}}] \geq \mathbb{E}_{T_1}[\tau_{T_1,S}^{\text{base}}] = \tau_1^{\text{base}}$ , with strict inequality if  
536  $\theta_{T_1,s}^{\text{delay}} > \theta_{T_1,s}^{\text{base}}$  on a set of nodes with positive probability. Finally, delay implies  
537 a smaller technology stock (higher  $L_{T_1,s}$ ) because learning-by-doing accumulates  
538 more slowly when early mitigation is zero. By (A9),  $L_{T_1,s}^{\text{delay}} \geq L_{T_1,s}^{\text{base}}$ , and since mit-  
539 igation costs are increasing in  $L_t$ ,  $\kappa_{T_1,s}(m_{T_1,s}, L_{T_1,s}^{\text{delay}}) \geq \kappa_{T_1,s}(m_{T_1,s}, L_{T_1,s}^{\text{base}})$ . Hence  
540 the total resource cost under delay is weakly higher, reinforcing the conclusion  
541 that  $\tau_1^{\text{delay}} \geq \tau_1^{\text{base}}$ .  $\square$

Table A1—: OLS estimate of the delay-to-price elasticity

	(1)
$L$ (years)	0.002761
	(0.000487)
Constant	5.241717
	(0.004929)
$R^2$	0.969818
Observations	3

Note: Dependent variable:  $\log(\tau_L^{\text{delay}})$ . Robust standard errors in parentheses. 95% confidence interval for the slope: [0.001806, 0.003715], i.e. [0.181%, 0.372%] per year.

542

## REGRESSION RESULTS DELAY-TO-PRICE ELASTICITY

543

## A2. Analytical solutions

544

COBB-DOUGLAS LIMIT OF THE EZ AGGREGATOR AND THE FIRST PERIODIC  
545 COMPENSATION

546 Solving for the consumption-equivalent DWL of delay when  $\rho \neq 0$  is done in  
547 the main text. Here we consider the Cobb–Douglas case  $\rho = 0$  (i.e.  $\sigma = 1$ ).

548 As  $\rho \rightarrow 0$ , the Epstein–Zin aggregator  $U_0 = ((1 - \beta)c_0^\rho + \beta \text{CE}_1^\rho)^{1/\rho}$  converges  
549 to the geometric (Cobb–Douglas) form  $U_0 = c_0^{1-\beta} \text{CE}_1^\beta$ . Let the delayed path  
550 have first-period consumption  $c_0^D$  and continuation certainty equivalent  $\text{CE}_1^D$ .  
551 We scale the first-period consumption by  $(1 + \phi)$  and require the compensated  
552 delayed utility to equal the baseline utility  $U_0^*$ :  $U_0^* = ((1 + \phi)c_0^D)^{1-\beta} (\text{CE}_1^D)^\beta$ .  
553 Solving for  $\phi$  gives the closed-form consumption-equivalent transfer:

$$(A13) \quad \phi_{\text{CD}} = \left[ \frac{U_0^*}{(c_0^D)^{1-\beta} (\text{CE}_1^D)^\beta} \right]^{\frac{1}{1-\beta}} - 1.$$

554

## A3. Extended outputs

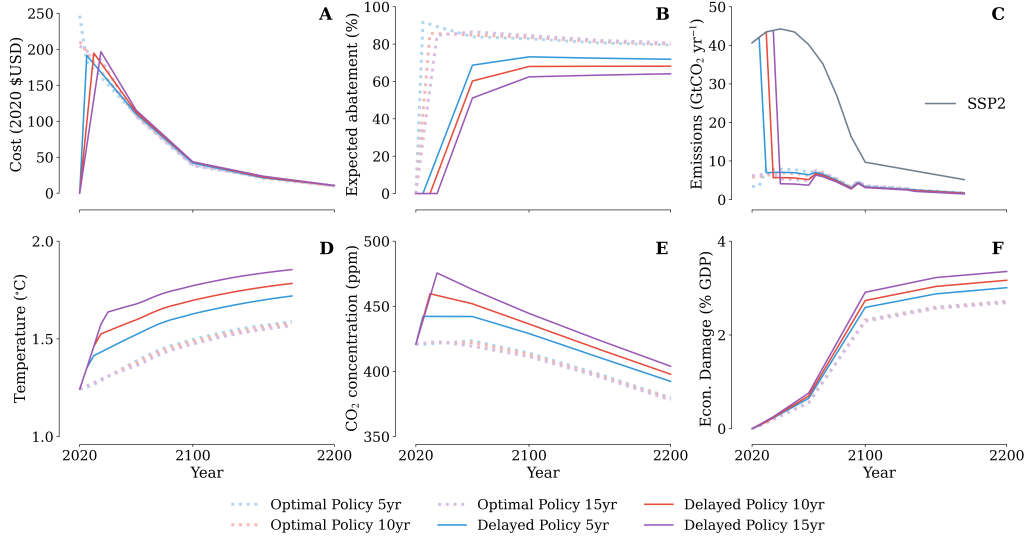
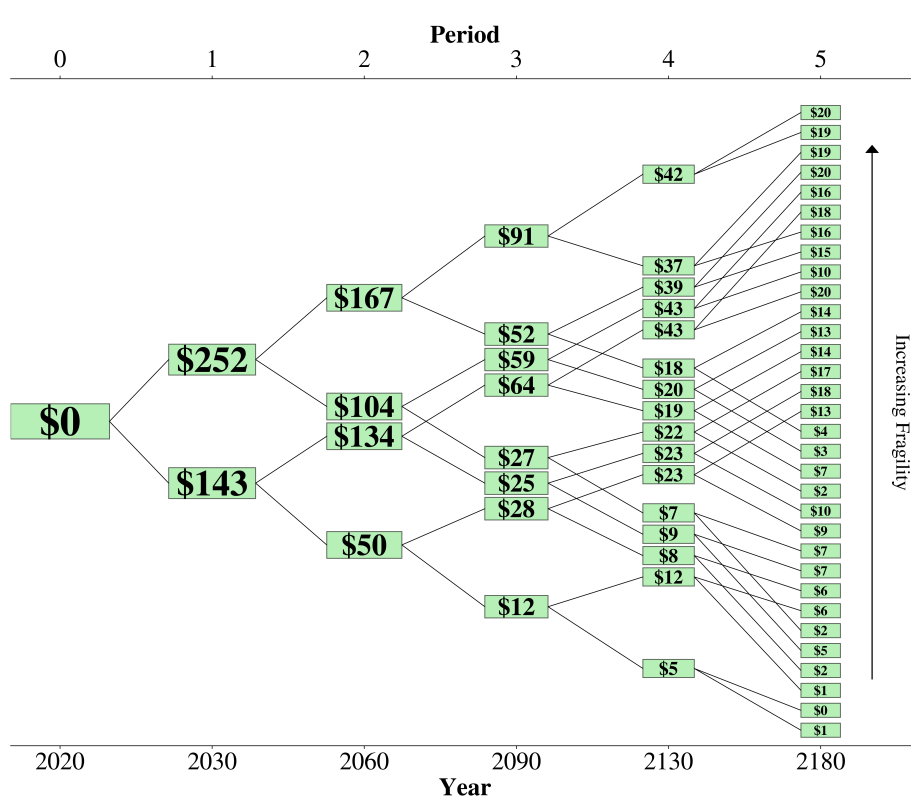
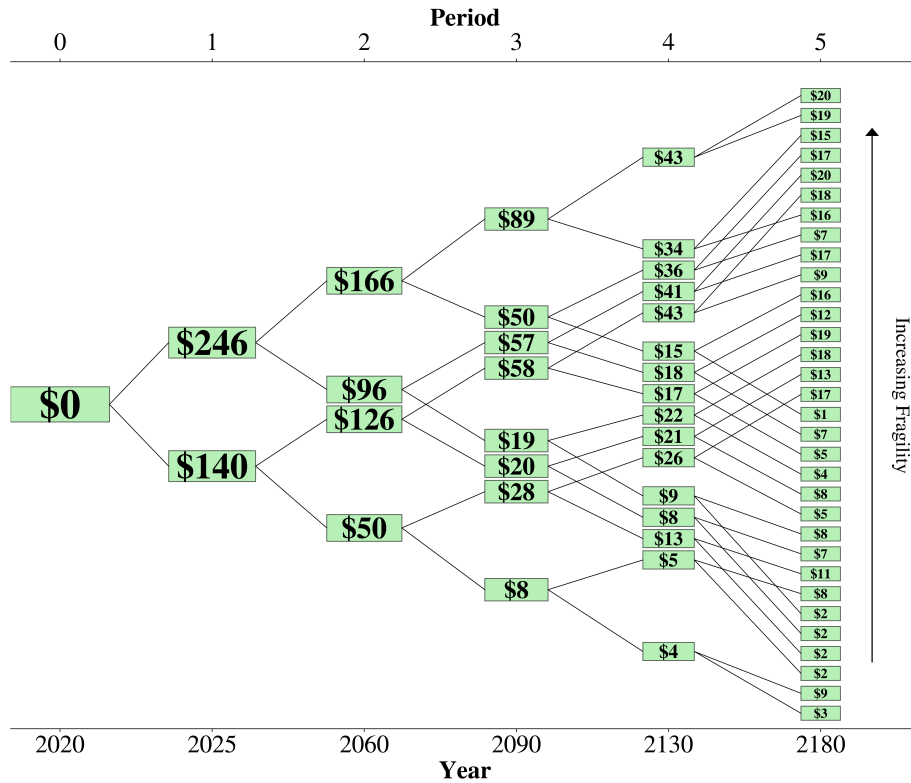


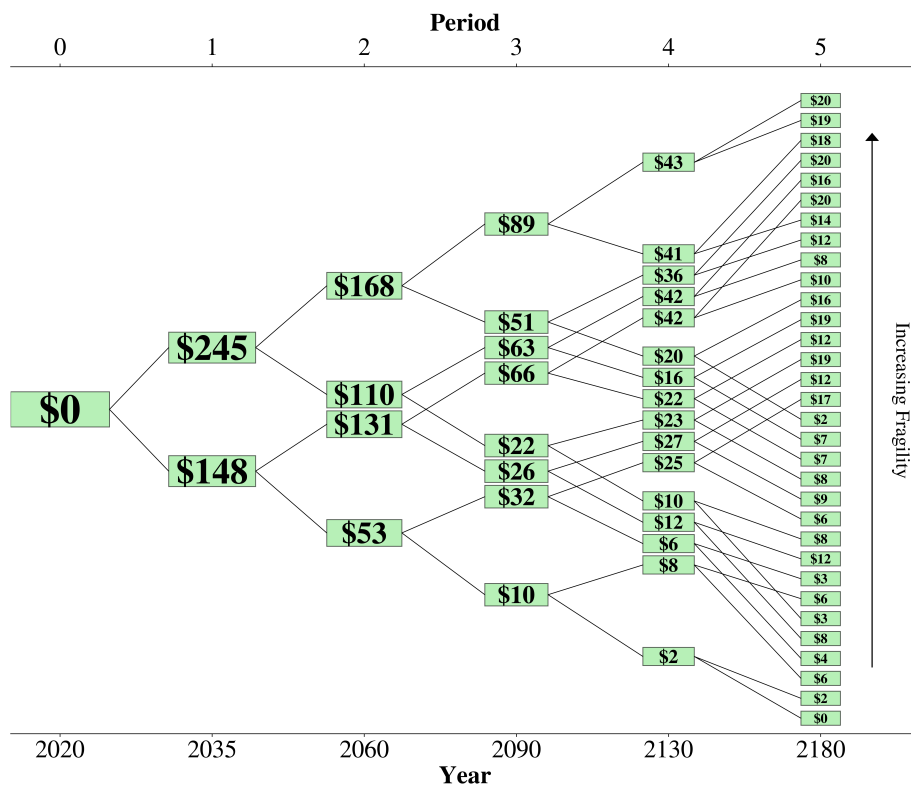
Figure A1. : Different outputs of the single-period optimal scenarios with delay periods  $L \in \{5, 10, 15\}$ .

*Note:* A: Expected carbon prices in 2020 \$/tCO<sub>2</sub>. B: Expected abatement in %. C: Emissions in GtCO<sub>2</sub>/year with SSP2 emissions baseline. D: Temperature in degrees Celsius. E: CO<sub>2</sub> concentration in ppm. F: Economic damages in % of Gross Domestic Product.



(b) Optimal price tree with 10-year delay.

Figure A2. : Decision trees for delayed runs.



(c) Optimal price tree with 15-year delay.

Figure A2. : Decision trees for delayed runs (continued).

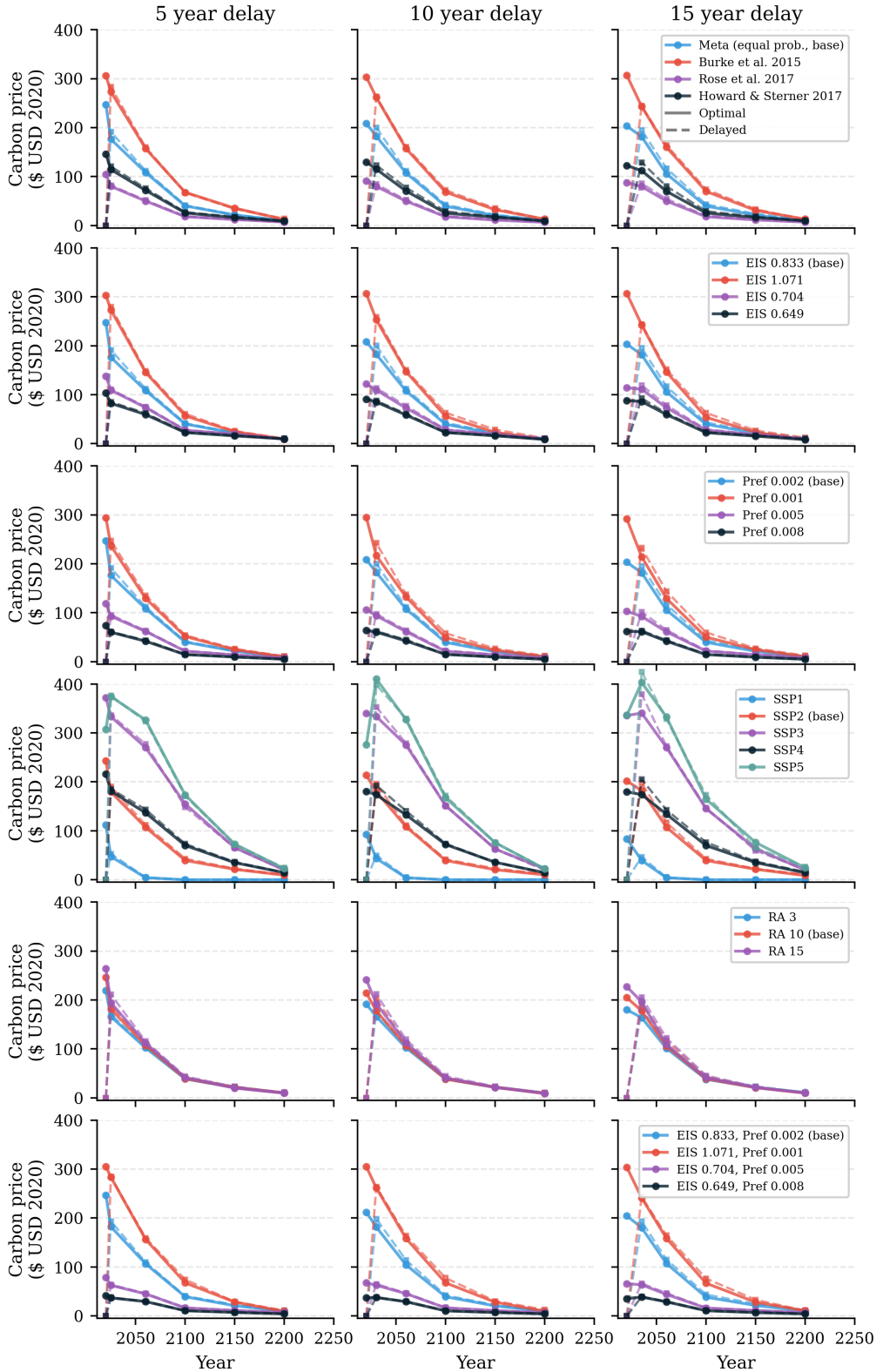


Figure A3. : Optimal carbon price paths under different parameter combinations.

*Note:* The legends call out the changed parameter in each row. All other parameters follow the main specification (base, see Appendix A.A1).

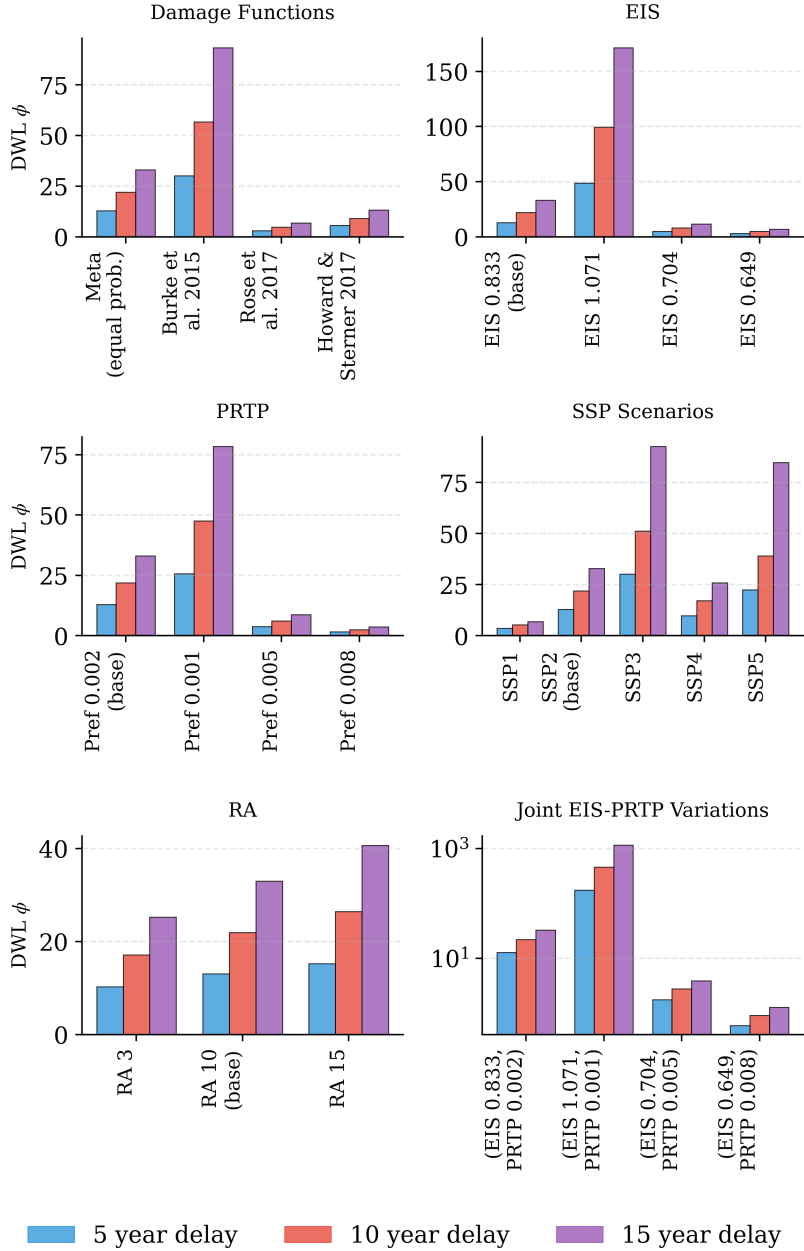


Figure A4. : DWL  $\phi$  (in %) under different parameter combinations.

*Note:* The x-axes describe the changed parameters for each graph. All other parameters follow the main specification (base, see Appendix A.1).